*drugs and drug candidates*

MDPI

*Article*

# An Investigation on the Relationships between Mass Spectrometric Collisional Data and Biological Activity/Stability of Some *N*-Acylethanolamine Acid Amidase (NAAA) β-Lactone Inhibitors

**Ilena Isak [1], Andrea Duranti [2,*] and Pietro Traldi [3]**

[1] SCION, Rotorua 3010, New Zealand
[2] Department of Biomolecular Sciences, University of Urbino Carlo Bo, 61029 Urbino, Italy
[3] Istituto di Ricerca Pediatrica, Fondazione Città della Speranza, 35127 Padova, Italy
* Correspondence: andrea.duranti@uniurb.it; Tel.: +39-0722-303501

**Abstract:** The rationale of the present study is that relationships between in vitro biological activity and mass spectrometric (MS) collisional data of molecular species have been already reported in the literature. Herein, the same approach has been employed to investigate possible correlations between MS stability and biological activity/stability data of a series of β-lactone amides and carbamates *N*-acylethanolamine acid amidase (NAAA) inhibitors. Electrospray ionization MS experiments were performed using an LCQ Deca ion trap and samples were introduced by direct infusion. Mass spectra of positive and negative ions have been obtained, and collisional experiments were performed on selected ionic species. Collisional-induced fragmentation pathways of molecular species related to β-lactone amide inhibitors are different in comparison to those of carbamates, being the former species more stable than the latter, due to β-lactone reactivity. Correlations were found between the characteristic collision energy ($CE_{50}$) obtained by the breakdown curves and in vitro NAAA inhibitory potency of the β-lactone amides and carbamates analyzed. In the case of carbamates, a relationship between $CE_{50}$ values and bovine serum albumin (BSA) stability data was also found, while any correlation was not found for amides due to their instability to BSA. β-Lactone NAAA inhibitors' activity can be qualitatively associated with their lability, as measured by $CE_{50}$ values. The results obtained could suggest that MS may be used as a preliminary experimental tool to identify carbamate NAAA inhibitors endowed with good biological stability.

**Keywords:** NAAA inhibitors; electrospray mass spectrometry; collisional experiments; characteristic collision energy; breakdown curves



**Citation:** Isak, I.; Duranti, A.; Traldi, P. An Investigation on the Relationships between Mass Spectrometric Collisional Data and Biological Activity/Stability of Some *N*-Acylethanolamine Acid Amidase (NAAA) β-Lactone Inhibitors. *Drugs Drug Candidates* **2023**, *2*, 109–120. https://doi.org/10.3390/ddc2010007

Academic Editor: Jean Jacques Vanden Eynde

Received: 13 January 2023
Revised: 22 February 2023
Accepted: 24 February 2023
Published: 2 March 2023



## 1. Introduction

*N*-acylethanolamine acid amidase (NAAA) [1,2] is an N-terminal cysteine nucleophile that belongs to the choloylglycine hydrolase family and is localized in lysosomes. It is highly active at acidic pH and responsible to deactivate palmitoylethanolamide (PEA), an endogenous fatty acid ethanolamide that exerts potent anti-inflammatory and analgesic effects [3–8].

In recent years, interest in NAAA has increased, owing to studies demonstrating that local administration of NAAA inhibitors to inflamed tissues, where PEA biosynthesis is downregulated, is effective in restoring the physiological levels of PEA [9–11]. In this scenario, classes of NAAA inhibitors such as α-acylamino-β-lactone are very promising tools in the field of inflammation and analgesia due to their ability to restore PEA levels after exposure to stimuli pro-inflammatory [9,11].

Human NAAA (*h*-NAAA) was characterized by matrix–assisted laser desorption/ionization (MALDI) mass spectrometry (MS), suggesting the formation of a non-covalent complex of α- and β-subunits [12]. High–resolution liquid chromatography–tandem mass spectrometry

(HRLC-MS/MS) has been employed by West et al. [13] and Armirotti et al. [14] to demonstrate that, after a recognition process at the substrate-binding site, N-terminal cysteine 131 acylation is the rapid, noncompetitive, and reversible mechanism of *h*-NAAA inhibition carried out by substituted β-lactones, *N*-benzyloxycarbonyl-L-serine β-lactone and (2*S*,3*R*)-2-methyl-4-oxo-3-oxetanylcarbamic acid 5-phenylpentyl ester (URB913 or ARN077), a molecule able to inhibit NAAA with high potency and exert antinociceptive effects in rodent pain models [15–17].

In past investigations, interesting correlations were obtained between in vitro inhibitory potency and characteristic collision energy ($CE_{50}$) (i.e., the CE necessary to fragment 50% of the precursor ion population) values of some fatty acid amido hydrolase (FAAH) carbamate inhibitors. $CE_{50}$ were determined by means of collisional–activated decompositions of molecular species generated by electrospray ionization (ESI) operating in the negative [ESI (−)] and positive [ESI (+)] ion mode, which also provide useful indications as to the mechanism of FAAH inactivation [18–20]. Furthermore, a very intriguing investigation has been carried out in recent times to develop methods for the screening and confirmation of synthetic cannabinoids in biological fluids through the characterization of some molecules of the URB series both through HRMS (High–Resolution Mass Spectrometry) in experiments of electrospray ionization of positive and collisional ions on protonated ions, and via ultra-high performance liquid chromatography coupled with a triple quadrupole (UHPLC-MS/MS) [21].

Recently, the structure–activity and structure–property relationships of several *N*-(2-oxo-3-oxetanyl)amides [22] and *N*-(2-oxo-3-oxetanyl)carbamates [15,23] have been reported. It was found that carbamates are more potent NAAA inhibitors endowed with good stability towards the prototypical off-target protein bovine serum albumin (BSA) and rat plasma, which are well-established in vitro models for hydrolytic metabolism. Moreover, very interestingly in vivo studies carried out with some of the compounds analyzed in the present investigation have been shown to attenuate inflammation and tissue damage and improve recovery of motor function in mice subjected to spinal cord trauma (**2**, Table 1) [9] or prevent carrageenan-induced leukocyte infiltration inflammation after local administration in vivo (**1**, Table 1) [22].

In the last year, as evidence of the renewed interest in the class of molecules, amides **5** (URB866, Table 1) and **1** (URB894, Table 1) have been used as tools for exploratory experiments aimed at improving stability through the use of nanoparticle systems [24,25]. More specifically, the use of materials based on poly(lactic-co-glycolic acid) (PLGA) has been envisaged because of its specific properties [PLGA is a biocompatible and biodegradable polymer with modifiable degradation times based on the molecular weight and chemical composition (lactide/glycolide ratio)], thus becoming very important vectors for the delivery of drugs [24,25]. The studies were developed with the aim of exploring the antioxidant activity of the molecules examined also through the use, both as a comparison and in combination, of the phytochemical compound rutin, consisting of glucose, rhamnose, and quercetin as an aglycone fraction. In fact, it is often used as a reference molecule in the investigations considered, due to its antioxidant activity related to radical scavenger properties, which it was important to understand how they would be enhanced by the presence of NAAA inhibitors. The obtained results confirmed the rationale of using the co-encapsulation approach to obtain a novel antioxidant nanomedicine and an improvement in the properties of the chemical class of the α-acylamino-β-lactone NAAA inhibitors [24,25].

This scenario also assumes a greater significance because of the attempts to make the molecules of the class more stable through the introduction of suitable electrodonating groups such as methyl on carbon β of the lactone ring (derivatives of threonine) or the substitution of the amide with the carbamate or the insertion of a *tert*-butyl on the latter functional group. Although they have brought about considerable improvements in stability, they have not proved to be decisive with respect to the degradation problem [15].

**Table 1.** Chemical structures, MW, $IC_{50}$ values, and in vitro BSA stability values of amide (**1–6**) and carbamate (**7–12**) NAAA inhibitors.

| Compounds | Chemical Structure | MW | $IC_{50}$ (μM ± S.E.M.) | BSA $t_{1/2}$ (Min) | Ref. |
|---|---|---|---|---|---|
| **1** | 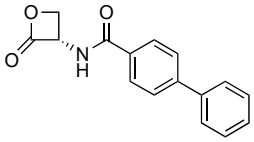 | 276.09 | 115 ± 13 | 3.3 ± 0.8 | [15,22] |
| **2** | 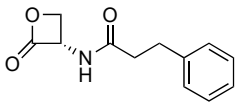 | 219.09 | 420 ± 20 | 7.0 ± 0.6 | [15,22] |
| **3** | 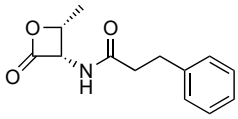 | 233.11 | >100 | 16.0 ± 1.2 | [15,22] |
| **4** | 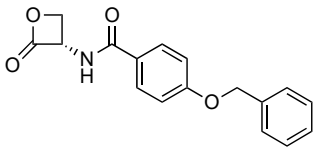 | 297.10 | 90 ± 10 | 5.8 ± 1.0 | [15,22] |
| **5** | 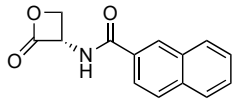 | 241.07 | 160 ± 40 | <1 | [15,22] |
| **6** | 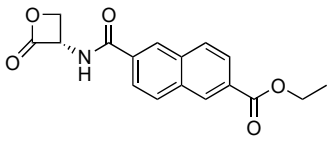 | 313.10 | 300 ± 20 | 3.2 ± 0.7 | [15,22] |
| **7** | 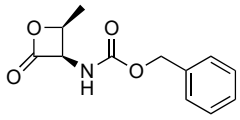 | 235.08 | 1 ± 0.2 | 5.1 ± 0.8 | [15] |
| **8** | 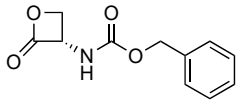 | 221.07 | 2.96 ± 0.30 | 1.2 ± 0.7 | [15] |
| **9** | 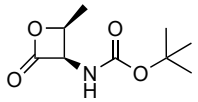 | 201.10 | 0.22 ± 0.03 | 129.1 ± 7.0 | [15] |
| **10** | 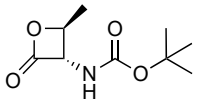 | 201.10 | 0.19 ± 0.04 | 87.7 ± 2.3 | [15] |
| **11** | 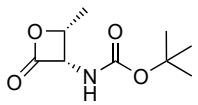 | 201.10 | >80 | 120.7 ± 1.1 | [15] |
| **12** | 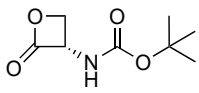 | 187.08 | 0.58 ± 0.20 | 19.6 ± 1.5 | [15] |

On the basis of those results, we attempted to establish whether energetic data generated by collision experiments could offer some insights into NAAA inhibitory potency

and, in particular, the off-target biological stability (BSA esterases) of selected amides and carbamates previously designed and studied [15,22].

## 2. Results and Discussion

*N*-(2-Oxo-3-oxetanyl)amides (**1–6**) and *N*-(2-oxo-3-oxetanyl)carbamates (**7–12**) NAAA inhibitors are reported in Table 1 together with some other their characteristics, such as chemical structures, molecular weight (MW), $IC_{50}$ (half-maximal concentration at inhibiting recombinant rat NAAA activity) values and in vitro BSA stability values. All molecules are characterized by a four-membered β-lactone ring, which is essential for the inhibition of NAAA but makes the molecule unstable and prone to be hydrolyzed by the opening of the lactone moiety. Some compounds (**3**, **7**, **9–12**) have a methyl group, which makes the molecules more chemically stable by enrichment of the partially positively charged electron cloud of the lactone carbon [22]. A further difference, apart from the presence of the carbamic moiety vs. the amide moiety, is due to substituents with different characteristics linked to the central group. Indeed, the steric and electronic bulk characteristics are different up to the *tert*-butyl group (**9–12**), which has resulted in greater chemical and metabolic stability (**9–11**), being compromised in the case of **12** by the absence of the methyl group [15].

All amide and carbamate NAAA inhibitors were analyzed in ESI conditions, operating in both negative and positive ionization modes, and only similar ionic species were taken into account for further consideration. Collisional experiments were performed on the molecular species to verify if there are relationships between MS stability data and the biological activity/stability of examined compounds. As an example, the production spectrum of the $[M–H]^-$ species of compound **10** is shown in Figure 1.

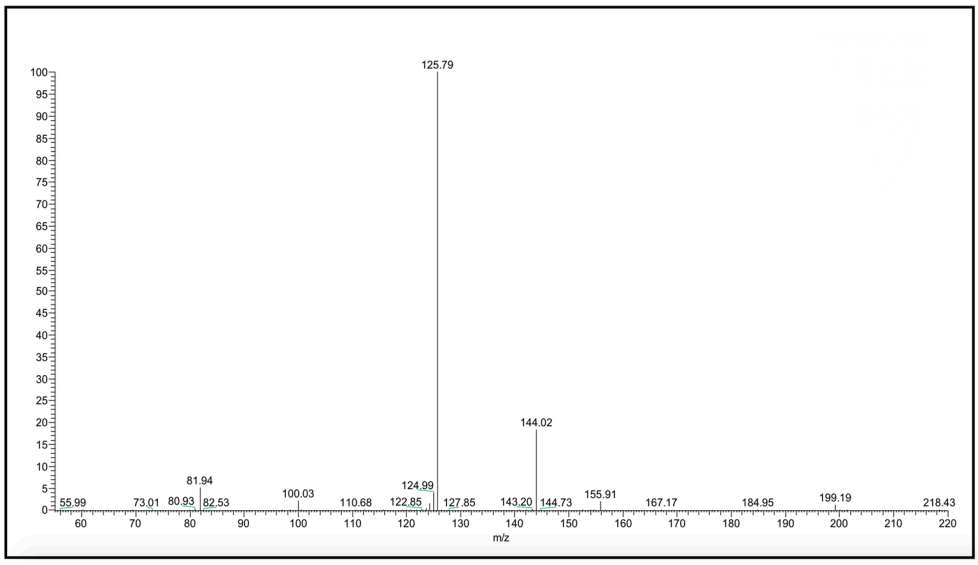


**Figure 1.** $[M–H]^-$ MS/MS spectrum of carbamate **10**.

Compound **10** shows a characteristic fragmentation. The fragment ion at *m*/*z* 144 is due to the loss of the *tert*-butylic group and that at *m*/*z* 126 is due to the loss of *tert*-buthoxy one (Figure 2).

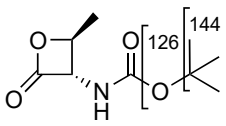


**Figure 2.** Representation of the collisional-induced fragment ions of **10** compounds.

In the negative ionization mode, deprotonated molecules were detected for all compounds. The $[M-H]^-$ ions of compounds **1–5** show an analogous behavior under collisional conditions, due to the cleavage of the β-lactone ring with further loss of $CO_2$ (route to ion "a", Scheme 1). Compound **6** shows a specific behavior, due to the loss of a neutral moiety of 46 u, which can be ascribed to EtOH by the cleavage of the ester bond (route to ion "c", Scheme 1). The fragmentation route to ion "c" can be well justified by its high stability. Compound **2** exhibits, in addition to the common $CO_2$ loss, a primary loss of $CH_2O$, reasonably originated from the cleavage of the β-lactone ring. In this case, the formation of a five-membered ring can be hypothesized, as shown in route to ion "b" of Scheme 1.

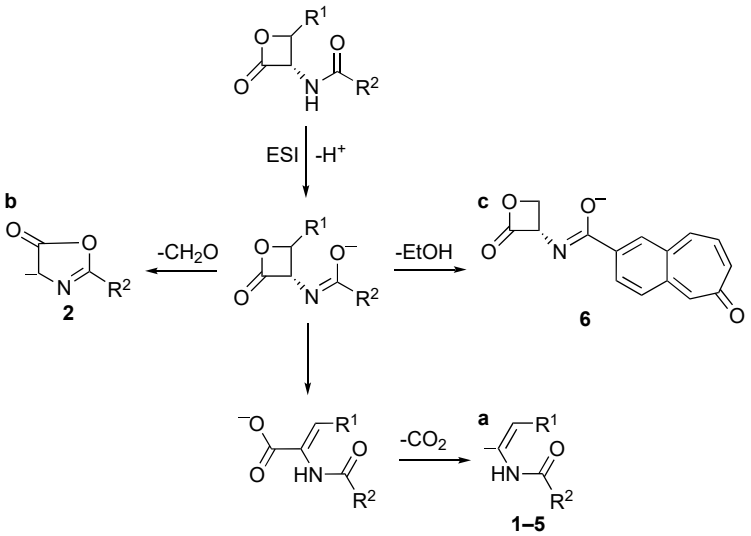


**Scheme 1.** Collisional-induced fragmentation pathways of amides **1–6** $[M–H]^-$ ions.

In positive ion ESI conditions compounds **1–6** led to $[MH]^+$ species. However, compounds **1**, **2**, and **4–6** $[MNa]^+$ ions are also detectable. The collisional-induced fragmentation of $[MH]^+$ ions mainly consists of primary losses of CO (route to ion "d", Scheme 2) and HCOOH (route to ion "e", Scheme 2), indicating an easy cleavage of the β-lactone ring. The decomposition route to ion "e" is observed for all compounds except **4**. On the contrary, CO loss is present for compounds **3–5** only.

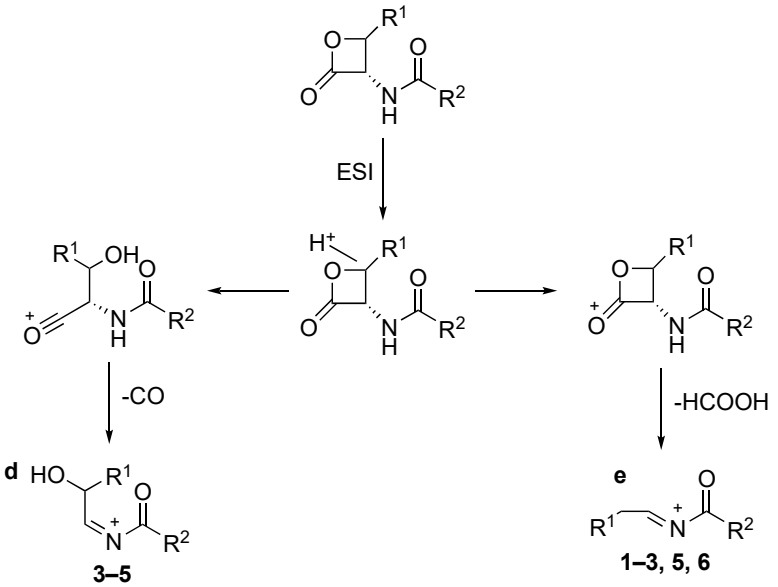


**Scheme 2.** Collisional-induced fragmentation pathways of amides **1–6** $[MH]^+$ ions.

Both negative and positive ion data indicate that either in acidic or basic media, the β-lactone ring is the most reactive moiety of molecules **1–6**. Consequently, it is conceivable that their activity and stability might be somehow related to the opening of the lactone ring as proposed in Schemes 1 and 2 for the $[M–H]^-$ and $[MH]^+$ species, confirming the results reported in the literature [14,22].

Conversely, $[M–H]^-$ ions of carbamate inhibitors **7–12** follow under collisional conditions and different decomposition pathways (Scheme 3). In this case, the most favored one is ascribed to the loss of $R^2OH$, leading to fragments "f" of Scheme 3. $[R^2–H]$ loss is observed, giving rise to ions "i" (compounds **9–12**). The primary $CO_2$ loss present in the fragmentation pattern of amides **1–6** is also observed in the case of compound **7** (ion "h") but with a lower yield. Loss of $CH_2O$ is observed in the case of compound **8** only, via cleavage of the β-lactone and rearrangement to ion "g".

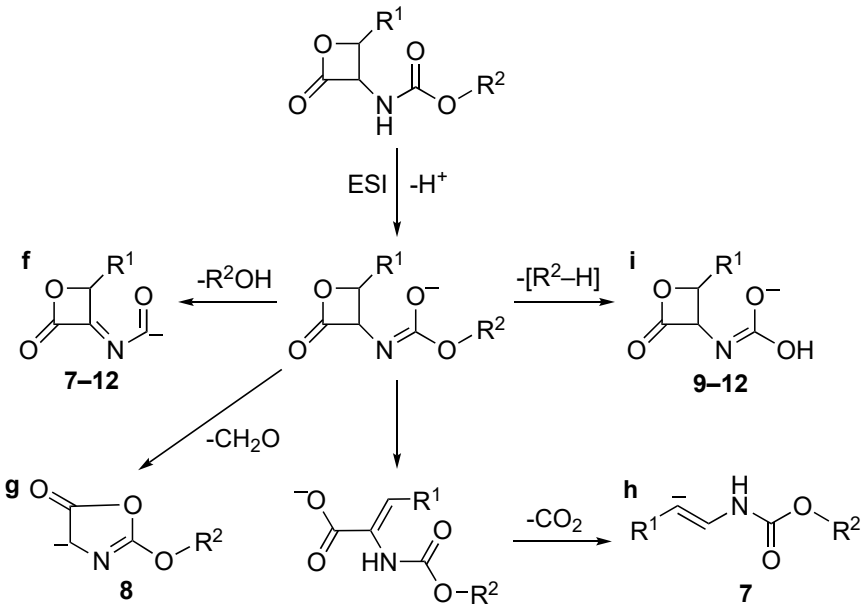


**Scheme 3.** Collisional-induced fragmentation pathways of carbamates **7–12** $[M–H]^-$ ions.

Therefore, collisional experiments performed on $[M–H]^-$ ion of compounds **1–12** show the occurrence of different fragmentation pathways, indicating that the β-lactone ring of amides (**1–6**) is more labile than that of carbamates (**7–12**).

Contrary to what was observed for **1–6**, sodiated ions are typical of carbamate **7–12** in positive ion conditions. Collisional experiments of $[MNa]^+$ ions show that, similarly to what was observed in negative conditions, the β-lactone moiety is conserved or rearranged depending on the substituent group, as shown in Scheme 4. The collisional-induced fragmentation patterns suggest the presence of $[MNa]^+$ ions of two different types, in which the $Na^+$ is chelated by the oxygen atoms of the β-lactone ring (compounds **9–12**, route to ion "k", Scheme 4) or by the ester oxygen atoms (compounds **7** and **8**, routes to ions "j" and "l", respectively, Scheme 4). The two routes justify the loss of $[R^2–H]$ or $CO_2$ and $C_3H_4O_2$.

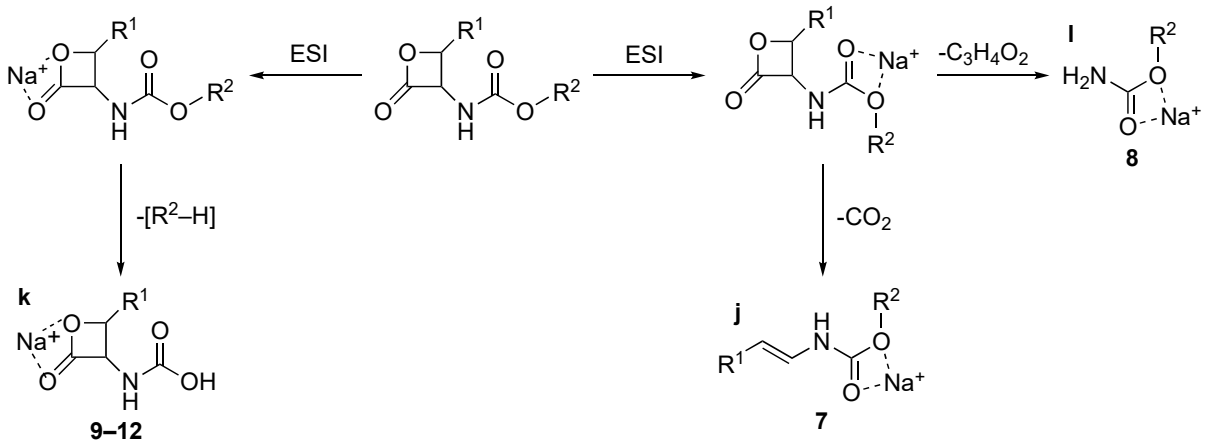


**Scheme 4.** Collisional-induced fragmentation pathways of carbamates **7–12** $[MH]^+$ ions.

The abundance of the collisional–generated ions from the molecular ionic species of **1–12** is reported in Table 2.

**Table 2.** $[M–H]^-$, $[MH]^+$, and $[MNa]^+$ fragment ions ("a–l") abundance of compounds **1–12**.

| Compounds | 1° Fragment Ion Abundance | 2° Fragment Ion Abundance | 1° Fragment Ion Abundance | 2° Fragment Ion Abundance |
|---|---|---|---|---|
| | ESI (−) | | ESI (+) | |
| **1** | 100% [a] | – | 100% [e] | – |
| **2** | 100% [a] | 70% [b] | 100% [e] | – |
| **3** | 100% [a] | – | 100% [d] | 50% [e] |
| **4** | 100% [a] | – | 100% [d] | – |
| **5** | 100% [a] | – | 100% [d] | 60% [e] |
| **6** | 100% [c] | – | 100% [e] | – |
| **7** | 100% [f] | 50% [h] | 100% [j] | – |
| **8** | 70% [f] | 100% [g] | 100% [l] | – |
| **9** | 100% [f] | 20% [i] | 100% [k] | – |
| **10** | 100% [f] | 20% [i] | 100% [k] | – |
| **11** | 100% [f] | 20% [i] | 100% [k] | – |
| **12** | 100% [f] | 50% [i] | 100% [k] | – |

It is to emphasize that collisional experiments performed by ion trap privilege the formation of low critical energy decomposition pathways, due to the step-by-step energy deposition mechanism. This behavior reflects the activation of the energetically most favored decomposition routes. Then, the collisional–generated reactions may be regarded as an extremely simplified model of an enzymatic reaction, but only when steric or other factors do not play a major role or these factors are constant in the considered series of compounds and can be averaged out.

The fragmentation pathways obtained by collisional experiments permit us to evaluate the critical energies of the different fragmentation channels of the protonated (or sodiated) and deprotonated molecules studied and highlight the most reactive points. They can be detected by varying the supplementary RF voltage, responsible for the collisional activation, thus obtaining highly reproducible plots (breakdown curves) of the variation of precursor and fragment ion abundances as a function of CE (see, for example, Figure 3).

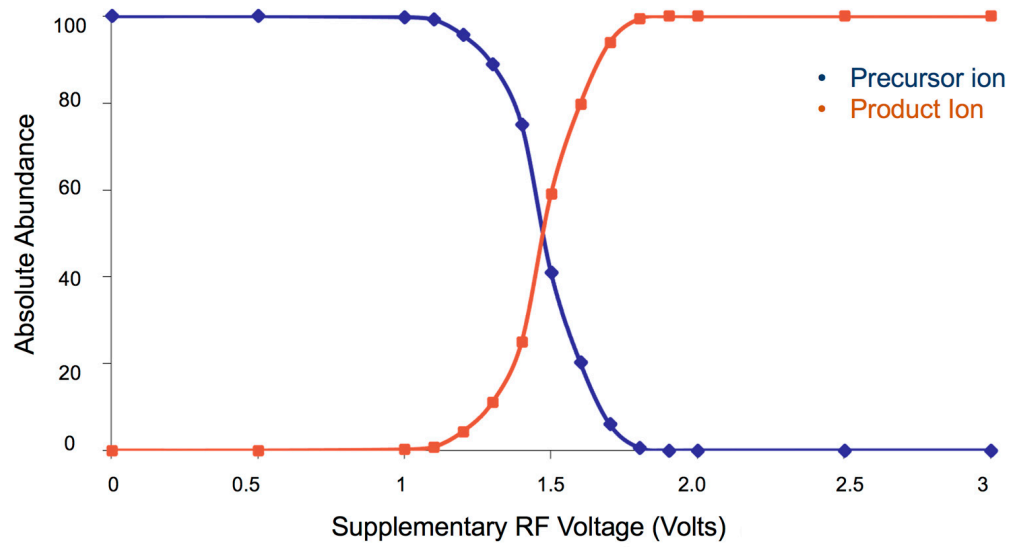


**Figure 3.** Breakdown curve obtained by collision of carbamate **10** $[M–H]^-$ molecular species. The data have been obtained by collision of $[M–H]^-$ species of compound **10** ($m/z$ 200) with the formation of ion "f" of Scheme 3. The related abundance has been calculated by varying the collision energy in the range of 0–3 V of supplementary RF voltage.

Breakdown curves highlight the differences in the decomposition energy of various preselected species. In particular, considering the $CE_{50}$ between the plots of the precursor and the fragment ions abundances, it is possible to obtain a value closely related to the critical energy of the decomposition processes.

It has been shown above that several fragmentation pathways are activated by collisions of $[M–H]^-$, $[MH]^+$, and $[MNa]^+$ ions of compounds **1–12**, and the breakdown curves related to the same product ions can be related to the energy associated with the characteristic route of fragmentation.

The $CE_{50}$ values relative to the $CO_2$ loss of $[M–H]^-$ ions of compounds **1–5** have been determined and found in the range of 1.10–1.95 V (Table 3). A similar determination has not been possible for compound **6**, due to the lack of $[M–H]^- \rightarrow [M–H–CO_2]^-$ fragmentation pathway (Scheme 1).

**Table 3.** Characteristic collision energy ($CE_{50}$) values of compounds **1–12** obtained for $[M–H]^-$ and $[MH]^+$ generated in ESI (−) and (+) ion mode.

| Compounds | Crossing Point ESI (−) | Crossing Point ESI (+) |
|---|---|---|
| | RF (Volts) | RF (Volts) |
| **1** | 1.95 ± 0.00 | 1.64 ± 0.01 |
| **2** | 1.42 ± 0.01 | 1.51 ± 0.04 |
| **3** | 1.29 ± 0.01 | 1.44 ± 0.01 |
| **4** | 1.10 ± 0.00 | 1.67 ± 0.03 |
| **5** | 1.15 ± 0.05 | 1.28 ± 0.08 |
| **6** | – | 1.63 ± 0.01 |
| **7** | 0.93 ± 0.01 | 1.13 ± 0.00 |
| **8** | 0.95 ± 0.00 | 1.16 ± 0.01 |
| **9** | 1.04 ± 0.00 | 0.86 ± 0.01 |
| **10** | 1.05 ± 0.00 | 0.96 ± 0.01 |
| **11** | 1.05 ± 0.00 | 1.03 ± 0.01 |
| **12** | 1.06 ± 0.01 | 0.95 ± 0.01 |

$[MH]^+$ ions of **1**, **2**, and **6** amides decompose exclusively through loss of HCOOH (Scheme 2) and the related $CE_{50}$ values are in the range of 1.51–1.64 V (Table 3). In the

case of **3** and **5** compounds, two concurrent decomposition pathways are present, due to losses of HCOOH and CO (Scheme 2) so the energy associated with the two decomposition pathways is lower than that observed for **1**, **2**, and **6** amides (1.44 and 1.28, respectively) (Table 3). In fact, the highest $CE_{50}$ value (1.67 V) is detectable from the $[MH]^+$ of compound **4**, characterized by only one loss of CO.

$[M–H]^-$ ions of derivatives **7–12** decompose mainly by reaction at the carbamate moiety (Scheme 3) and fragment "f" is the most relevant uniformly observed one (Scheme 3 and Table 2). The $CE_{50}$ values range between 0.93 and 1.06 V (Table 3), indicating the need for a different energy for compounds bearing benzyl vs. *t*-butyl, groups, and the higher lability of carbamates **7–12** in comparison to the amide derivatives 1–6 (1.10–1.95 V). Noteworthy is the fact that, differently from compounds **1–6**, the β-lactone ring is conserved in the case of **7–12** molecules. This can explain the different $CE_{50}$ values observed between amide and carbamate derivatives.

Compounds **7–12** show in ESI (+) conditions the privileged formation of $[MNa]^+$ ions, which decompose through the routes reported in Scheme 4. In this case, fragments related to the cleavages of both the β-lactone ring and the ester moiety are observed. The $CE_{50}$ values for **9–12** carbamates related to fragment "k" are in the range of 0.86–1.03 V (Table 3), pointing to the particular lability of the carbamate moiety. For compounds **7** and **8** the $CE_{50}$ values are slightly higher, probably because the fragmentation involves the β-lactone moiety.

The described data indicate quite clearly that the reactivity of the β-lactone NAAA inhibitors analyzed is very different, being higher in the case of the amide vs. carbamate compounds on the basis of the $CE_{50}$ values (Table 3). This is dependent on a different mode of fragmentation carried out by amide and carbamate derivatives.

We then examined whether $CE_{50}$ values in the negative or positive mode could be related to NAAA $IC_{50}$ values of compounds analyzed (**1–12**). Even if the relationship between NAAA $IC_{50}$ and $CE_{50}$ could not be quantitatively confirmed when compounds **1–12** were all included [$r^2$ = 0.233 in the case of data from ESI (−) and $r^2$ = 0.426 in the case of data from ESI (+)], it is interesting to observe that it improved considerably in ESI (−) if compound **1** is excluded ($r^2$ = 0.778). In our opinion, the behavior is probably due to the characteristics of the unique *p*-biphenyl substituent in compound **1** with respect to the others.

Previous investigation has established that carbamates **7–12** have higher potency and better BSA esterases stability than amides **1–6** (0.19–80 μM vs. 90–420 μM) and [max values 129.1 min (**9**) vs. 16.0 min (**3**)], respectively (Table 1) [15]. With respect to carbamate compounds, we observed a correlation between $CE_{50}$ values from ESI (−) and BSA stability [$r^2$ = 0.893] with compounds **9–11** (**7**, **8**, and **12** are not to be considered because of their low biological stability). As expected, no correlations are present in the case of amides **1–6** because they are not stable with BSA.

## 3. Materials and Methods

### *3.1. Chemicals*

Amides (**1–6**) and carbamates (**7–12**) were provided by the Department of Biomolecular Sciences of the University of Urbino Carlo Bo (Section of Chemistry and Pharmaceutical Technologies, Urbino, Italy). Their synthetic procedures and biological and chemical stability assay values have been described previously [15,22]. Methanol was purchased from Sigma Aldrich (Milan, Italy). Briefly, with regard to synthetic procedures, amides **1**, **2**, **4–6** were prepared by reaction of the corresponding acyl chloride and the tosylate (*S*)-2-oxo-3-oxetanylammonium toluene-4-sulfonate salts in the presence of triethylamine. In the case of **1**, **4**, and **6** a two-step synthesis was required starting from the corresponding carboxylic acids, which were converted into acyl chlorides with oxalyl chloride and a catalytic amount of dimethylformamide. The synthesis of threonine β-lactone **3** was carried out through a four-step procedure starting from L-threonine, whose protection and subsequent cyclization to β-lactone then allowed the deprotection of the amino group and adopted the same proto-

col previously described for other amides. The synthetic procedure for carbamates **7**, **9–11** is briefly reported as follows. The amino groups of L-, D-, and L-*allo*-threonine were protected, and then the corresponding cyclization to β-lactones was accomplished by treating the parent compounds with *N*-benzyloxycarbonyl (Cbz) chloride (in the case of the **7** intermediate) or di-*tert*-butyl dicarbonate ($Boc_2O$) (for **9–11**); subsequently, the compounds obtained reacted with benzotriazol-1-yloxytris(dimethylamino)phosphonium hexafluorophosphate (BOP reagent). Compound **8** was synthesized by initial protection of the L-serine with Cbz followed by hydroxy acid cyclization via a modified Mitsunobu reaction. Finally, this type of reaction was also followed by **12** starting from *N*-*tert*-butyloxycarbonyl-L-serine.

### *3.2. Instrumental Analysis*

ESI experiments were performed using an LCQ Deca (Thermo Finnigan, San Jose, CA, USA) ion trap operating in positive and negative ion modes. Compounds were dissolved in MeOH:$H_2O$ (50:50, *v*/*v*), and their $10^{-6}$ M solutions were directly infused into the ESI source at 10 μL/min. The ions were produced using spray voltage, capillary voltage, and entrance capillary temperature of ±4 kV, ±8 V, and 220 °C, respectively. MS/MS experiments were performed by resonant excitation of the ions through a supplementary radio frequency (RF) voltage in the range 10–50% of its maximum value (5 V peak-to-peak) with ion accumulation time of 400 ms and isolation width set at 2 mass units. Compounds were analyzed in triplicate and the results are expressed as mean ± standard deviation.

### *3.3. Biochemical Assays*

Rat NAAA $IC_{50}$ and stability towards BSA values were reported previously [15,22].

## 4. Conclusions

Although probably not considered a univocal and/or resolutive means in all circumstances, MS makes an important contribution in terms of investigations aimed at predicting biological activity and offers the advantage of very limited costs compared to those necessary to carry out biological assays. The present investigation indicates that NAAA inhibitory activity can be qualitatively correlated with the reactivity of compounds analyzed as measured by their $CE_{50}$ values. A correlation is obtained between the energetic data achieved by collisional experiments carried out with carbamates and their in vitro biological stability in the BSA model. This could suggest that MS, such as in the case of FAAH inhibitors [18–20], may be used as an experimental diagnostic tool to identify carbamate NAAA inhibitors endowed with good biological stability and as promising molecules for topical anti-inflammatory use as soft drugs [15,17], antinociceptive [16], and/or antioxidant drugs [24,25].

**Author Contributions:** Conceptualization, I.I., A.D. and P.T.; methodology, I.I. and P.T.; formal analysis, I.I.; investigation, I.I., A.D. and P.T.; resources, A.D. and P.T.; data curation, I.I. and P.T.; writing–original draft preparation, I.I., A.D. and P.T.; writing–review and editing, I.I., A.D. and P.T.; supervision, P.T.; funding acquisition, A.D. and P.T. All authors have read and agreed to the published version of the manuscript.

**Funding:** This research was funded by the University of Urbino Carlo Bo and Istituto di Ricerca Pediatrica, Fondazione Città della Speranza, Padova.

**Institutional Review Board Statement:** Not applicable.

**Informed Consent Statement:** Not applicable.

**Data Availability Statement:** Not applicable.

**Conflicts of Interest:** The authors declare no conflict of interest.

## References


1. Tsuboi, K.; Sun, Y.X.; Okamoto, Y.; Araki, N.; Tonai, T.; Ueda, N. Molecular characterization of N-acylethanolamine-hydrolyzing acid amidase, a novel member of the choloylglycine hydrolase family with structural and functional similarity to acid ceramidase. *J. Biol. Chem.* **2005**, *280*, 11082–11092. [CrossRef] [PubMed]
2. Ueda, N.; Tsuboi, K.; Uyama, T. N-acylethanolamine metabolism with special reference to N-acylethanolamine–hydrolyzing acid amidase (NAAA). *Prog. Lipid Res.* **2010**, *49*, 299–315. [CrossRef] [PubMed]
3. Lo Verme, J.; Fu, J.; Astarita, G.; La Rana, G.; Russo, R.; Calignano, A.; Piomelli, D. The nuclear receptor peroxisome proliferator-activated receptor-α mediates the anti-inflammatory actions of palmitoylethanolamide. *Mol. Pharmacol.* **2005**, *67*, 15–19. [CrossRef] [PubMed]
4. Hu, J.; Ying, H.; Yao, J.; Yang, L.; Ma, H.; Li, L.; Zhao, Y. Micronized palmitoylethanolamide ameliorates methionine and choline deficient diet-induced nonalcoholic steatohepatitis via inhibiting inflammation and restoring autophagy. *Front. Pharmacol.* **2021**, *12*, 744483. [CrossRef]
5. Beggiato, S.; Tomasini, M.C.; Ferraro, L. Palmitoylethanolamide (PEA) as a potential therapeutic agent in Alzheimer's disease. *Front. Pharmacol.* **2019**, *10*, 821. [CrossRef]
6. D'Amico, R.; Impellizzeri, D.; Cuzzocrea, S.; Di Paola, R. ALIAmides update: Palmitoylethanolamide and its formulations on management of peripheral neuropathic pain. *Int. J. Mol. Sci.* **2020**, *21*, 5330. [CrossRef]
7. Clayton, P.; Hill, M.; Bogoda, N.; Subah, S.; Venkatesh, R. Palmitoylethanolamide: A natural compound for health management. *Int. J. Mol. Sci.* **2021**, *22*, 5305. [CrossRef]
8. Fotio, Y.; Jung, K.-M.; Palese, F.; Obenaus, A.; Tagne, A.M.; Lin, L.; Rashid, T.I.; Pacheco, R.; Jullienne, A.; Ramirez, J. NAAA-regulated lipid signaling governs the transition from acute to chronic pain. *Sci. Adv.* **2021**, *7*, eabi8834. [CrossRef]
9. Solorzano, C.; Zhu, C.; Battista, N.; Astarita, G.; Lodola, A.; Rivara, S.; Mor, M.; Russo, R.; Maccarrone, M.; Antonietti, F.; et al. Selective N-acylethanolamine-hydrolyzing acid amidase inhibition reveals a key role for endogenous palmitoylethanolamide in inflammation. *Proc. Natl. Acad. Sci. USA* **2009**, *106*, 20966–20971. [CrossRef]
10. Bottemanne, P.; Muccioli, G.G.; Alhouayek, M. N-acylethanolamine hydrolyzing acid amidase inhibition: Tools and potential therapeutic opportunities. *Drug Discov. Today* **2018**, *23*, 1520–1529. [CrossRef]
11. Piomelli, D.; Scalvini, L.; Fotio, Y.; Lodola, A.; Spadoni, G.; Tarzia, G.; Mor, M. N-acylethanolamine acid amidase (NAAA): Structure, function, and inhibition. *J. Med. Chem.* **2020**, *63*, 7475–7490. [CrossRef]
12. West, J.M.; Zvonok, N.; Whitten, K.M.; Wood, J.T.; Makriyannis, A. Mass spectrometric characterization of human N-acylethanolamine-hydrolyzing acid amidase. *J. Proteome Res.* **2012**, *11*, 972–981. [CrossRef]
13. West, J.M.; Zvonok, N.; Whitten, K.M.; Vadivel, S.K.; Bowman, A.L.; Makriyannis, A. Biochemical and mass spectrometric characterization of human N-acylethanolamine-hydrolyzing acid amidase inhibition. *PLoS ONE* **2012**, *7*, e43877. [CrossRef]
14. Armirotti, A.; Romeo, E.; Ponzano, S.; Mengatto, L.; Dionisi, M.; Karacsonyi, C.; Bertozzi, F.; Garau, G.; Tarozzo, G.; Reggiani, A.; et al. β-Lactones inhibit N-acylethanolamine acid amidase by S-acylation of the catalytic N-terminal cysteine. *ACS Med. Chem. Lett.* **2012**, *3*, 422–426. [CrossRef]
15. Duranti, A.; Tontini, A.; Antonietti, F.; Vacondio, F.; Fioni, A.; Silva, C.; Lodola, A.; Rivara, S.; Solorzano, C.; Piomelli, D. N-(2-Oxo-3-oxetanyl)carbamic acid esters as N-acylethanolamine acid amidase inhibitors: Synthesis and structure–activity and structure–property relationships. *J. Med. Chem.* **2012**, *55*, 4824–4836. [CrossRef]
16. Sasso, O.; Moreno-Sanz, G.; Martucci, C.; Realini, N.; Dionisi, M.; Mengatto, L.; Duranti, A.; Tarozzo, G.; Tarzia, G.; Mor, M.; et al. Antinociceptive effects of the N-acylethanolamine acid amidase inhibitor ARN077 in rodent pain models. *Pain* **2013**, *154*, 350–360. [CrossRef]
17. Sasso, O.; Summa, M.; Armirotti, A.; Pontis, S.; De Mei, C.; Piomelli, D. The N-acylethanolamine acid amidase inhibitor ARN077 suppresses inflammation and pruritus in a mouse model of allergic dermatitis. *J. Investig. Dermatol.* **2018**, *138*, 562. [CrossRef]
18. Basso, E.; Duranti, A.; Mor, M.; Piomelli, D.; Tontini, A.; Tarzia, G.; Traldi, P. Tandem mass spectrometric data–FAAH inhibitory activity relationships of some carbamic acid O-aryl esters. *J. Mass Spectrom.* **2004**, *39*, 1450. [CrossRef]
19. Valitutti, G.; Duranti, A.; Lodola, A.; Mor, M.; Piersanti, G.; Piomelli, D.; Rivara, S.; Tontini, A.; Tarzia, G.; Traldi, P. Correlation between energetics of collisionally activated decompositions, interaction energy and biological potency of carbamate FAAH inhibitors. *J. Mass Spectrom.* **2007**, *42*, 1624. [CrossRef]
20. Valitutti, G.; Duranti, A.; Mor, M.; Piersanti, G.; Piomelli, D.; Rivara, S.; Tontini, A.; Tarzia, G.; Traldi, P. The collisional behavior of ESI-generated protonated molecules of some carbamate FAAH inhibitors isosteres and its relationships with biological activity. *J. Mass Spectrom.* **2009**, *44*, 561. [CrossRef]
21. Agostini, M.; Favretto, D.; Renzoni, C.; Vogliardi, S.; Duranti, A. Characterization of URB series synthetic cannabinoids by HRMS and UHPLC–MS/MS. *Pharmaceuticals* **2023**, *16*, 201. [CrossRef]
22. Solorzano, C.; Antonietti, F.; Duranti, A.; Tontini, A.; Rivara, S.; Lodola, A.; Vacondio, F.; Tarzia, G.; Piomelli, D.; Mor, M. Synthesis and structure—Activity relationships of N-(2-oxo-3-oxetanyl)amides as N-acylethanolamine-hydrolyzing acid amidase inhibitors. *J. Med. Chem.* **2010**, *53*, 5770–5781. [CrossRef] [PubMed]
23. Ponzano, S.; Bertozzi, F.; Mengatto, L.; Dionisi, M.; Armirotti, A.; Romeo, E.; Berteotti, A.; Fiorelli, C.; Tarozzo, G.; Reggiani, A.; et al. Synthesis and structure—Activity relationship (SAR) of 2-methyl-4-oxo-3-oxetanylcarbamic acid esters, a class of potent N-acylethanolamine acid amidase (NAAA) inhibitors. *J. Med. Chem.* **2013**, *56*, 6917–6934. [CrossRef] [PubMed]

24. Gagliardi, A.; Molinaro, R.; Fresta, M.; Duranti, A.; Cosco, D. α-Acylamino-β-lactone N-acylethanolamine-hydrolyzing acid amidase inhibitors encapsulated in PLGA nanoparticles: Improvement of the physical stability and protection of human cells from hydrogen peroxide-induced oxidative stress. *Antioxidants* **2022**, *11*, 686. [CrossRef]
25. Gagliardi, A.; Voci, S.; Ambrosio, N.; Fresta, M.; Duranti, A.; Cosco, D. Characterization and preliminary in vitro antioxidant activity of a new multidrug formulation based on the co-encapsulation of rutin and the α-Acylamino-β-lactone NAAA inhibitor URB894 within PLGA nanoparticles. *Antioxidants* **2023**, *12*, 305. [CrossRef]